Microstructure of 5 keV gold-implanted polydimethylsiloxane

Muhamed Niklaus,[a,*] Samuel Rosset,[a] Massoud Dadras,[b]
Phillipe Dubois[a] and Herbert Shea[a]

[a]Ecole Polytechnique Fédérale de Lausanne (EPFL), Microsystems for Space Technologies Laboratory (LMTS),
Rue Jaquet-Droz 1, Case Postale 526, CH-2002 Neuchâtel, Switzerland
[b]Institute of Microtechnology, University of Neuchâtel, Neuchâtel, Switzerland

The first high-resolution transmission electron microscopy (TEM) cross-section images of flexible electrodes fabricated by gold ion implantation at 5 keV into polydimethylsiloxane (PDMS) are presented. A TEM sample preparation method based on cryo-ultramicrotomy, adapted for extremely low-modulus (1 MPa) elastomers, was developed, allowing the gold nanoparticles in a PDMS matrix to be imaged. The cluster size, size distribution and implantation depth of 50 nm were determined from the images and used to calculate the Young's modulus of the implanted layer.
© 2008 Acta Materialia Inc. Published by Elsevier Ltd. All rights reserved.

Keywords: Metal ion implantation; EAP; PDMS; Elasticity of nanocomposites; Gold clusters

Highly compliant electrodes capable of withstanding large strains (>0.4) are important for a number of applications, in particular for dielectric electroactive polymer (EAP) actuators, also known as artificial muscles, and for flexible electronics. When developing highly efficient milli- and micrometer-scale dielectric EAPs using PDMS as the elastomer, it has been shown that electrodes fabricated by metal ion implantation into the PDMS by filtered cathodic vacuum arc (FCVA) has several advantages over more common fabrication methods, such as incorporation of carbon or metal powder in the elastomer, coating with conductive grease or implanting with other conventional implanters [1–3]. These implanted electrodes (i) can be patterned on the micrometer scale (ii) remain conductive for stains of over 40% and (iii) yield the smallest possible increase in Young's modulus of the stack. The details on the use of low-energy (5 keV) Au and Ti ion implantation to create compliant electrodes on PDMS-based buckling mode actuators are reported in Ref. [4].

Metal ion implantation has been used primarily to modify surface properties [5,6] and has been applied to different polymers [7,8], but rarely to elastomers [9]. During ion implantation, the physical and mechanical properties of the polymer are modified through direct damage of the polymer and by the inclusion and growth of metallic nanoparticles. Gold implantation in PET was studied by Yuguang et al. [10]. They observed three different layers, consisting of: a destructured surface layer with low ion concentration; a buried layer of a high ion concentration with metallic clusters having very high conductivity; and a mostly undamaged layer with a low density of particles. In general, one might expect such a structure, but the boundaries, thicknesses and number of different levels have not hitherto been studied much.

The conduction mechanisms of physically modified (doped, implanted, etc.) insulators have been widely studied for different materials: oxides, glasses, composite materials, semiconductors and polymers [11–13]. The conduction mechanisms (tunneling, hopping, variable range hopping, percolation and thin film conductivity) in these composite systems are complex. Depending on the implantation conditions, any one of these phenomena can be dominant. With regard to the mechanical properties, several numerical and analytical approaches have been reported to describe porous composites or composites with spherical inclusions [14–16]. Analytical models use global structural characteristics of the composites, e.g. size of the clusters, to predict the mechanical properties.

Existing models deal with composites as homogeneous over their entire volume. Consequently, in order

* Corresponding author. Tel.: + 41 327205182; fax: +41 327205754; e-mail: muhamed.niklaus@epfl.ch

to analyze the implanted PDMS films, which are 20 μm thick with only the top 50 nm layer containing metal nanoparticles, the implanted layer must be considered separately from the non-implanted layer. This can be challenging because the limit between different layers is not sharply defined.

In order to understand the microstructure resulting from the implantation, and to relate the microstructure (e.g. cluster size, distribution, grain growth and atom diffusion) to conduction mechanisms and macroscopic physical properties (Young's modulus, stress, conductivity), a direct observation of the microstructure is required. Standard TEM preparation methods cannot be used on soft polymer materials. In this article a TEM preparation method and micrographs are presented that allow determination of the implantation depth, cluster size and size distribution of gold implanted at 5 keV as a function of the dose. This information is used with an analytical formula to determine the mechanical properties of the implanted zone.

The samples consist of 20 μm thick PDMS films bonded on patterned silicon chips with 2 and 3 mm diameter through-holes. This structure allowed the bulge test to be used to measure the change in the membrane's Young's modulus and stress due to the implantation. Implantation is performed on one side of the membrane for the studies reported here and on both sides to create the actuators reported in Refs. [3,4,17]. Low-energy gold implantation was performed with an FCVA implanter with an average energy of 5 keV. TEM was performed with a Philips CM transmission electron microscope.

TEM lamellae were prepared using a cryoultramicrotome (Leica Ultracut E) at -130 ± 5 °C. A piece of the membrane was cut with a razor blade and clamped between two polystyrene plates. Using the same temperature for the probe, knife and chamber, lamellae were sliced with a 35° diamond knife at a sectioning speed of 0.6 mm s^{-1}. With a perfect loop the slices were transferred from the blade to a carbon-coated TEM grid (200 mesh). The lamellae are stretched due to the surface tension of the water, and are nearly uncompressed. With a section thickness setting of 60 nm, a yellow interference color with the optical microscope was observed, corresponding to approximately 80 nm thickness. Two nearly identical preparation techniques were developed: (i) one for the bare film, which allowed for nanoparticles to be at the edge (thinnest part) of the lamella, and hence the best image sharpness of the metal nanoparticles; and (ii) one for a coated film, where an additional 20 μm thick layer of PDMS was spun over the implanted layer (Fig. 1). In the first method the relative position of the metal nanoparticles in the lamellae was not preserved, while in the second method the relative position of the particles is preserved but at the expense of image sharpness, since the nanoparticles are then at the middle of the sample and hence at the thickest part of the lamella.

Figure 2 is a plot of measured Young's modulus and surface resistivity vs. implanted gold dose in the PDMS films. As the dose increases, the film stiffness increases and the resistance drops. By increasing the dose, the particle size increases and the intercluster spacing decreases (see Fig. 5), up to the point where a conductive network
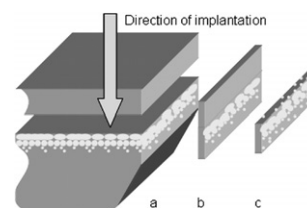

Figure 1. Two preparation techniques. (a) A trimmed block of an implanted sample with an optional subsequently coated layer of PDMS on the top. (b) TEM lamellae prepared with the additional layer of PDMS. (c) TEM lamellae of the bare film.
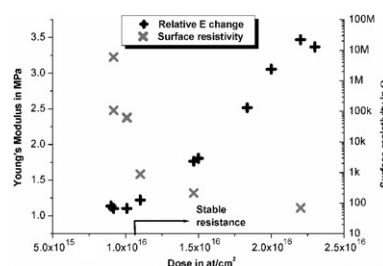

Figure 2. Measured mechanical and electrical properties of PDMS for the 5 keV gold implantation.

is formed. This domain is characterized by an abrupt decrease in the resistivity and is referred to as the percolation threshold, occurring here at a dose of 1×10^{16} at cm^{-2}. Above this dose a continuous metallic layer starts to form and the electrical properties vary only moderately with concentration, approaching those of a thin film. The evolution of the mechanical properties is explained in a similar fashion, and the sensitivity of the Young's modulus in the percolation domain confirms this phenomenon (Fig. 2).

Three doses, 0.9×10^{16}, 1.5×10^{16} and 2.3×10^{16} at cm^{-2}, were chosen for the TEM observations as they are situated around the area of interest, with the dose being high enough to obtain sufficiently conductive layers but low enough not to reach the mechanical properties of a metallic film. For these three samples the Young's modulus increases by 30–308% (initial value 0.85 MPa) and the resistivity varies from 270 kΩ/sq to 173 Ω/sq.

Simulations of gold concentration vs. depth in the PDMS for these three doses is obtained using the program TRIDYN [18] (Fig. 3). Dynamical progression of the ion concentration reveals a peak shift toward
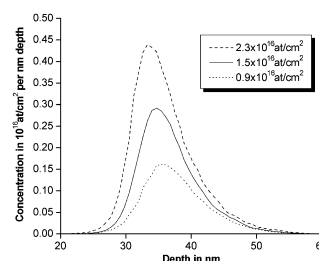

Figure 3. Simulated (TRYDIN) depth profiles of Au in PDMS for three doses of Au at 5 keV.

the surface and, as expected, a non-Gaussian distribution due to the continuous modification of material. The straggle becomes smaller at the higher doses, readily explained by the increasing concentration of the implanted gold particles inside the PDMS stopping incoming ions more effectively than PDMS.

Figure 4 presents TEM micrographs of the PDMS implanted at the three doses, obtained using the "coated" sample preparation method. The ions agglomerate into small clusters whose size increases with the dose forming at 2.3×10^{16} at cm^{-2} a dense ion-polymer composite structure that appears as a continuous metallic film.

The surface roughness as observed in the cross-section is in very good agreement with the topology measured by AFM, confirming that this lamella preparation method preserves the initial distribution of the particles. The surface of the implanted PDMS film is difficult to distinguish, and is located at the top of the nanoparticle layer (i.e. the nanoparticles are at most a few nanometers below the surface). This discrepancy with the simulation will be discussed below. The penetration depth of the ions does not exceed 50 nm, consistent with the simulation.

Three aspects of the FCVA implant process are important for determining the location of the nanoparticles: (i) the distribution of ion charge states (ii) the time evolution of the applied bias and (iii) sputtering. Of the gold ions, 10% are simply charged, 75% doubly charged and 5% triply charged [19]. The 2.5 keV bias drops rapidly during each implant pulse due to conduction through the plasma. Also, since the PDMS is an insulator, charge builds up during each pulse, thereby reducing the effective bias. There is thus a large spread in ion energies.

Figure 5 shows two TEM micrographs of PDMS samples implanted at doses of (a) 9×10^{16} at cm^{-2} and (b) 2.3×10^{16} at cm^{-2} prepared with the "uncoated" technique, allowing greater imaging sharpness on thinner lamellae, but spreading out the nanoparticles over 100–200 nm. This allows them to be imaged in detail and their size distribution to be measured (Fig. 6).
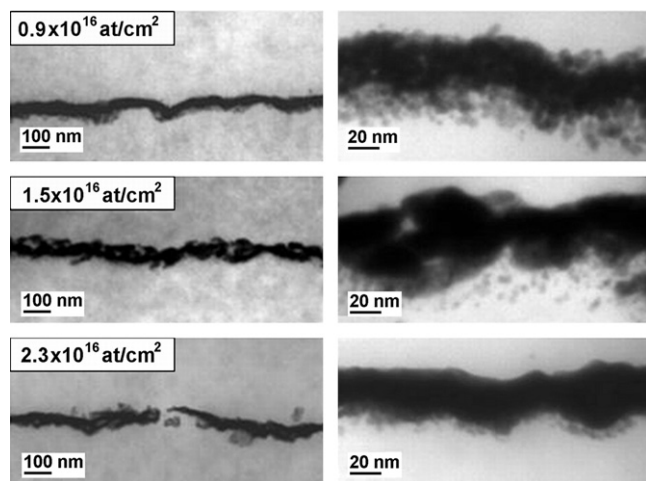

Figure 4. TEM cross-section micrograph PDMS samples implanted with Au ions at 5 keV. Ions were implanted from the top.
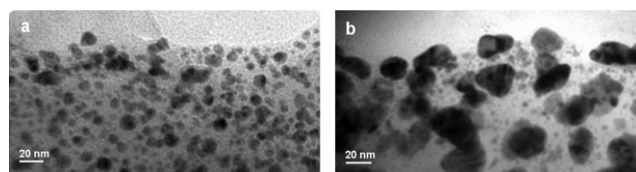

Figure 5. TEM cross-section micrograph of gold implanted PDMS samples prepared without any additional PDMS film for ion doses of: (a) 0.9×10^{16} at cm^{-2} and (b) 2.3×10^{16} at cm^{-2}.
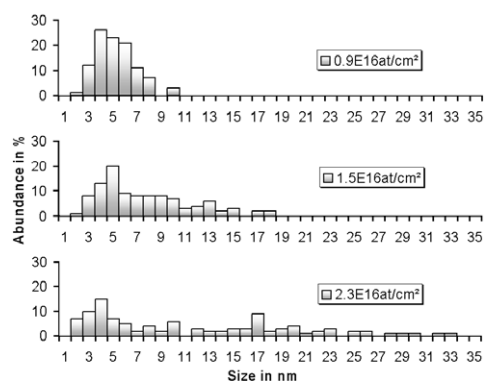

Figure 6. Histograms of the cluster sizes for the three gold ion doses indicated based on the TEM micrographs, using 300 particles for each dose.

The TEM dark-field mode and the corresponding diffraction patterns clearly showed gold crystalline particles and demonstrated that the nanoparticles are not amorphous.

The reason for the difference in the TEM images between Figures 4 and 5 is the preparation method. The gold clusters behave like solid particles, not bound to the polymer. During sectioning the knife moves the particles from their initial position and redistributes them over several hundreds of nanometers. The additional PDMS layer used for the samples in Figure 4 prevented removal of the clusters from the surface, but made the lamellae thicker.

The cluster size increases with the dose. At higher gold concentrations the mean free path of ions decreases, favoring the growth of bigger crystalline structures. The measured size distribution of the particles is not Gaussian (Fig. 6). A steep rise in abundance is seen for small clusters up to 5 nm size for all three doses. The higher the dose, the lower the abundance of 5 nm particles, presumably because small particles merge at higher doses.

Models relating the physical macroscopic properties of composites to the microscopic structure assume a homogeneously structured composite, not a composite film on top of a single-element substrate. The models can therefore only be applied to the thin implanted layer, not the 20 μm thick PDMS film implanted on the top.

The simple laminar theory predicts the properties of a composite according to the volume fraction of each constituent [20]. The Voigt model is geometrically well suited for our mechanical measurements and gives the average modulus for the case when the constituents

Table 1. Comparison of measured and computed Young's modulus for three gold ion doses (D)

D (at cm^{-2})	$V_{Au,20\mu m}$ (%)	$V_{Au,50nm}$ (%)	E_m (MPa)	$E_{T20\mu m}$ (MPa)	E_{C50nm} (MPa)
2.3×10^{16}	0.02	7.8	3.4	15.7	1025
1.5×10^{16}	0.01	5.1	1.8	8.6	385
0.9×10^{16}	0.008	3.1	1.1	7.1	105

are mixed in parallel layers (i.e. isostrain conditions) according to the following formula: $E_T V_T = E_{Au} V_{Au} + E_P V_P$, where E is the Young's modulus, V is the volume fraction, and the subscripts T, Au and P refer to composite, gold and PDMS constituents.

Table 1 compares the measured Young's modulus (E_m) with the predictions of the Voigt formula ($E_{T20\mu m}$) when applied to the full PDMS film thickness. $E_{T20\mu m}$ is 4–7 times bigger than E_m because the model assumes a 1.5–73.9 nm thick film of gold on a 20 μm membrane, rather than the same amount of gold in clusters distributed over 50 nm.

The same linear model can be used to compute E_{C50nm}, the Young's modulus of the 50 nm thick top layer of the membrane that contains all the implanted ions, using $E_m = E_{C50nm} V_{C50nm} + E_P V_P$, where $V_{C50nm} = 0.25\%$ ($= 50$ nm/20 μm). The gold volume fraction ($V_{Au,50nm}$) of the 50 nm layer can be calculated directly from the dose. The two main parameters, $V_{Au,50nm}$ and E_{C50nm}, of the thin layer containing all the implanted metal can thus be determined and used for the modeling of the mechanical and electrical properties of the gold ion implanted PDMS.

The more precisely the position of the clusters can be determined, for example, by dividing the composite into several sublayers characterized by different concentrations or structure (e.g. damaged polymer, clusters or film), the more accurate the results will be.

The measurements were performed on 20 μm thick films, the computation were for both the full film thickness and for the top 50 nm layer. $V_{Au,20\mu m}$, $V_{Au,50nm}$, $E_{T20\mu m}$ and E_{C50nm} are the volume fractions of Au and computed Young's modulus of a 20 μm thick membrane and a 50 nm thick composite.

This article presents the first TEM cross-section of PDMS membranes implanted with high doses (10^{16} ions cm^{-2}) of low-energy gold ions. These membranes are used as highly compliant electrodes in polymer actuators. The TEM images allowed the gold nanoparticles size and separation to be analyzed, and confirm the crystallinity of the clusters. At 5 keV gold ions reach a maximum penetration depth of 50 nm and aggregate into nanoparticles. The dependence of the clusters' size, structure and distribution on the dose was measured, and the microstructure was related to the electrical and mechanical properties. The Young's modulus for the implanted layer was computed. This study opens the door for the application of the different models in order to describe the properties of the composite and to better control the fabrication of lightweight and efficient large-stroke microactuators.

[1] A. Pimpin, Y. Suzuki, N. Kasagi, MEMS'04, 2004.
[2] M. Niklaus, S. Rosset, P. Dubois, M. Dadras, R.H. Shea, Mater. Res. Soc. Symp. Proc. 1052 (2008).
[3] S. Rosset, M. Niklaus, P. Dubois, M. Dadras, H. Shea, SPIE Proc. 6524 (2007) 652410.
[4] S. Rosset, M. Niklaus, P. Dubois, H.R. Shea, Sens. Actuators A 144 (2008) 185.
[5] B. Pukanszky, Composites 21 (1990) 3.
[6] N. Bowden, S. Brittain, A.G. Evans, J.W. Hutchinson, G.M. Whitesides, Nature 393 (1998) 146.
[7] K. Dworecki, T. Hasewaga, K. Sudlitz, S. Wasik, Nucl. Instrum. Methods Phys. Res. B 166 (2000) 646.
[8] F. Husein, C. Chang, J. Mater. Sci. Lett. 21 (2002) 1611.
[9] I.F. Husein, C. Chan, S. Qin, P.K. Chu, J. Appl. Phys. D 33 (2000) 2869.
[10] W. Yuguang, Z. Tonghe, L. Andong, Z. Gu, Surf. Coat. Technol. 157 (2002) 262.
[11] H.G. Svavarsson, J.T. Gudmundsson, H.P. Gislason, Phys. Rev. B 69 (2004) 155209.
[12] Z.M. Elimat, J. Appl. Phys. D 39 (2006) 2824.
[13] K. Nozaki, T. Itami, J. Phys. Condens. Matter 18 (2006) 2191.
[14] T.W. Clyne, P.J. Withers, An Introduction to Metal Matrix Composites, Cambridge University Press, Cambridge, 1993.
[15] S. Torquato, Random Heterogeneous Materials: Microstructure and Macroscopic Properties, Springer, New York, 2002.
[16] R. McLaughlin, Int. J. Eng. Sci. 15 (1977) 237.
[17] P. Dubois, S. Rosset, S. Koster, J. Stauffer, S. Mikhaïlov, M. Dadras, N.-F. de Rooij, H. Shea, Sens. Actuator A 130 (2006) 147.
[18] W. Möller, W. Eckstein, J.P. Biersack, Comput. Phys. Commun. 51 (1988) 355.
[19] G. Brown, X. Godechot, IEEE Trans. Plasma Sci. 19 (1991) 713.
[20] I.M. Ward, J. Sweeney, An Introduction to the Mechanical Properties of Solidpolymers, 2nd ed., John Wiley & Sons, New York, 2004.